

Supplementary Information for

Fabrication of Nano-objects with Morphology-Related Room-Temperature Phosphorescence and Their Application in Information Encryption

Wen Xu, Depeng Yin, Caiyuan Pan, Chao Liu, Chunyan Hong**

CAS Key Laboratory of Soft Matter Chemistry, Department of Polymer Science and Engineering, University of Science and Technology of China, Hefei, Anhui 230026, China

*E-mail: liuchao216@ustc.edu.cn; hongcy@ustc.edu.cn

Materials

Benzyl methacrylate (BzMA, 98%) was purchased from TCI (Shanghai, China) and purified by passing through a column of Al₂O₃ to remove the inhibitor prior to use. α -Methoxy- ω -hydroxy poly(ethylene oxide) with molecular weight M_n of 2000 (PEO₄₅-OH) was purchased from TCI (Shanghai, China) and used as received. 4-Cyano-4-(2-phenylethanesulfanyl-thiocarbonyl)sulfanylpentanoic acid was prepared according to the literature.¹ *N, N'*-Azobis (isobutyronitrile) (AIBN, Energy Chemical Reagent Co.) was purified by recrystallization from ethanol. 2-Bromoethanol, 4-bromo-2,5-dihydroxybenzaldehyde and methacryloyl chloride were purchased from TCI (Shanghai, China) and used without further purification. Dichloromethane (DCM), ethanol and tetrahydrofuran

(THF) were bought from Shanghai Chemical Reagent Co. and used as received. All other reagents with analytical grade were bought from Aladdin Reagent of China and used as received.

Measurements

^1H NMR spectra were recorded on a Bruker 400 MHz spectrometer in CDCl_3 and DMSO-d_6 , and tetramethylsilane (TMS) was used as an internal reference.

The molecular weights and molecular weight distributions of polymers were measured by GPC containing a Waters 1515 HPLC pump equipped with an RI detector and ultra-styragel columns ($500, 10^3, 10^4 \text{ \AA}$) calibrated with monodisperse polystyrene (PS) standards. THF was used as the eluent at a flow rate of 1.0 mL/min.

The photoluminescence (PL) spectra were recorded on the Hitachi F-4600 fluorescence spectrophotometer. The phosphorescence decays and relative phosphorescence quantum yields of the polymer nano-objects were obtained on the Fluorolog-3-Tau spectrofluorometer. The excitation wavelength was set as 365 nm. The concentration of polymer nano-objects was 0.5 mg/mL, and the dispersion was deoxygenated by three freeze-pump-thaw cycles unless specifically mentioned. The UV-vis spectra were recorded on the Shimadzu UV-2700 spectrophotometer.

Synthesis of cross-linker (CL)

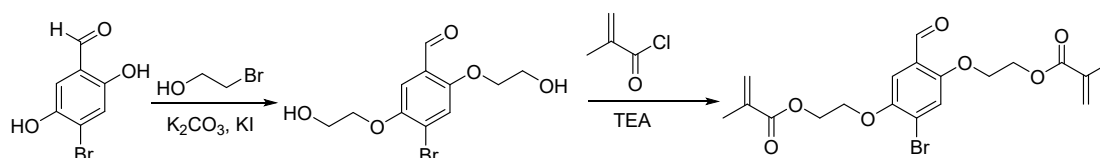


Figure S1. The synthetic procedure of the cross-linker (CL).

CL was prepared according to the previous literature.² The synthetic procedure of CL is shown in **Figure S1**. The 1H NMR spectrum of CL is given in **Figure S2**.

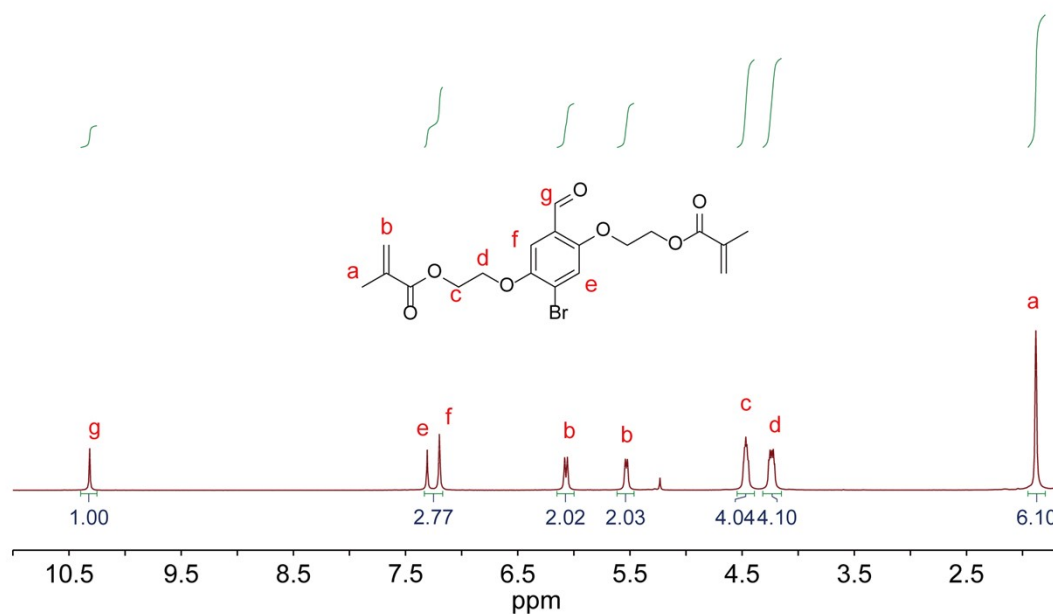


Figure S2. The 1H NMR spectrum of CL in $CDCl_3$.

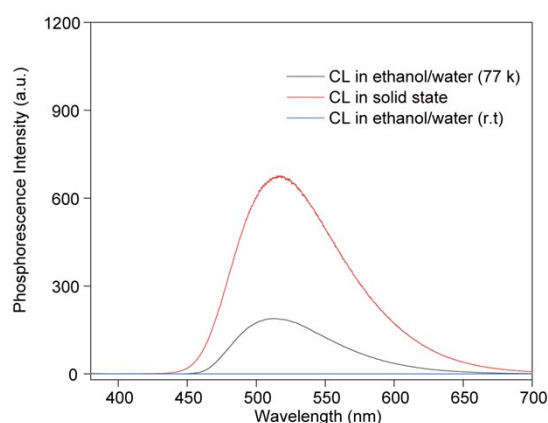


Figure S3. The phosphorescence emission spectra of CL at different states. The concentration of CL in ethanol/water mixture was 5 mg/mL and the solution was deoxidized. The phosphorescence spectrum of CL solid powder was obtained in the air.

Synthesis of macroCTA PEO₄₅-PETTC

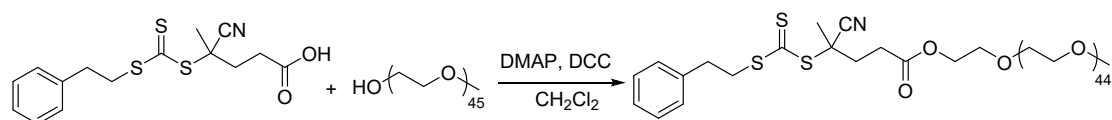


Figure S4. Synthesis of macroCTA PEO₄₅-PETTC.

The synthetic route of PEO₄₅-PETTC is shown in **Figure S4**. Poly(ethylene oxide)₄₅ (5.0 g, 2.5 mmol), 4-cyano-4-(2-phenylethanesulfanylthiocarbonyl)sulfanylpentanoic acid (3.39 g, 10.0 mmol), and 4-(dimethyl amino) pyridine (0.1 g, 1.0 mmol) were added into 75 mL of anhydrous CH₂Cl₂ in a 250 mL round-bottom flask. Dicyclohexylcarbodiimide (2.1 g, 10.0 mmol) dissolved in anhydrous CH₂Cl₂ (25 mL) was added dropwise into the flask at 0 °C. The reaction was kept stirring at room temperature

for 3 days, and then the mixture was filtered to remove *N, N'*-dicyclohexylurea. PEO₄₅-PETTC was obtained as yellow powder in 88% yield by precipitation in diethyl ether for three times and dried under vacuum overnight. The ¹H NMR spectrum of PEO₄₅-PETTC is shown in **Figure S5** and the GPC curve for PEO₄₅-PETTC is displayed in **Figure S6**.

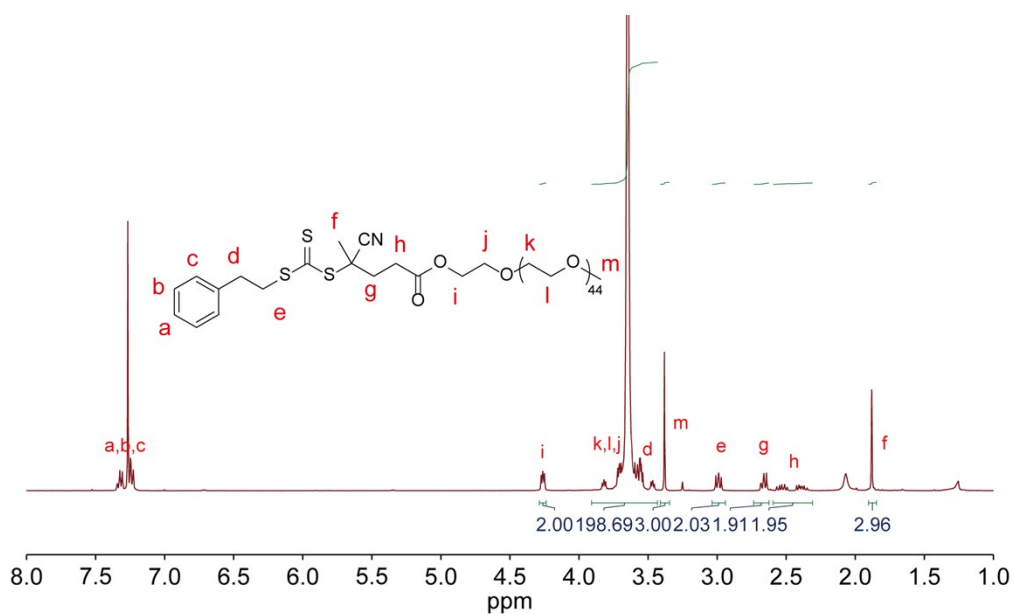


Figure S5. The ¹H NMR spectrum of PEO₄₅-PETTC in CDCl₃.

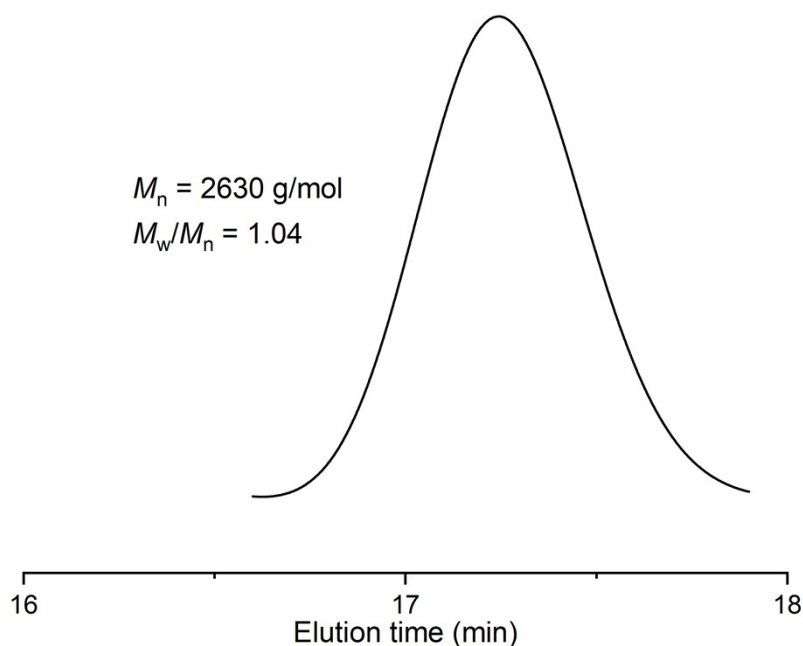


Figure S6. The GPC curve of PEO₄₅-PETTC with THF as the eluent.

Synthesis of PEO₄₅-*b*-P(BzMA-*co*-CL) polymer nanoparticles via RAFT dispersion copolymerization

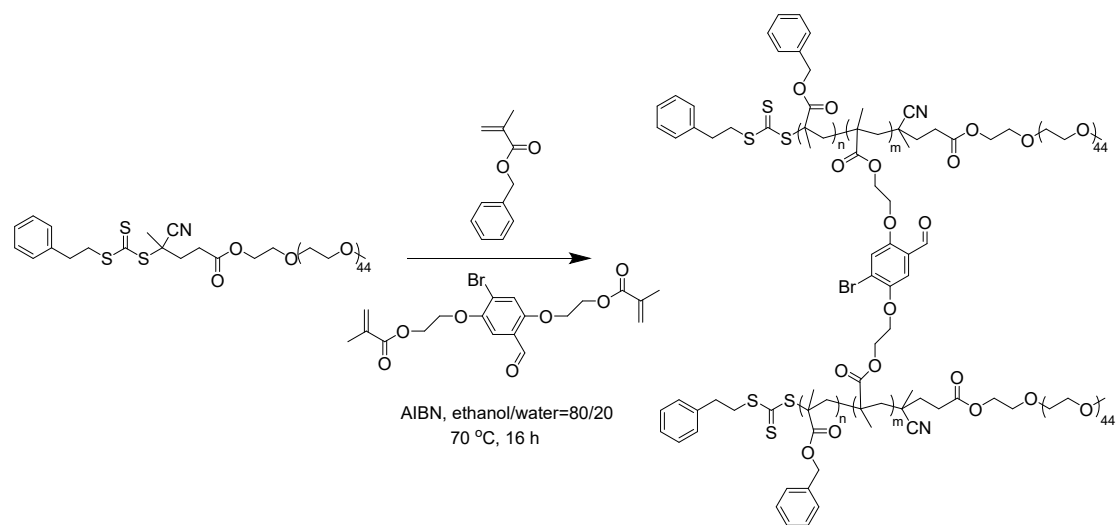


Figure S7. The synthetic route of PEO-*b*-P(BzMA-*co*-CL) nano-objects through RAFT dispersion copolymerization.

The typical synthetic procedure of PEO₄₅-*b*-P(BzMA_{*x*}-*co*-CL₂) nanoparticles is depicted as follows: in a 2 mL glass tube with a magnetic bar, PEO₄₅-PETTC (10.5 mg, 4.0 μmol), AIBN (0.1 mg, 0.6 μmol), BzMA

(56.4 mg, 0.3 mmol), CL (3.5 mg, 7.9 μmol) and ethanol/water mixture (w/w = 80/20, 400 mg) were added, and then the glass tube was degassed by three freeze-pump-thaw cycles to remove oxygen and sealed under vacuum. The polymerization was performed at 70 $^{\circ}\text{C}$ for 16 h. For GPC analysis, the mixture was dried in vacuum to give the solid powder, then the solid powder was dissolved in THF and precipitated in petroleum ether for three times to afford the pure copolymers.

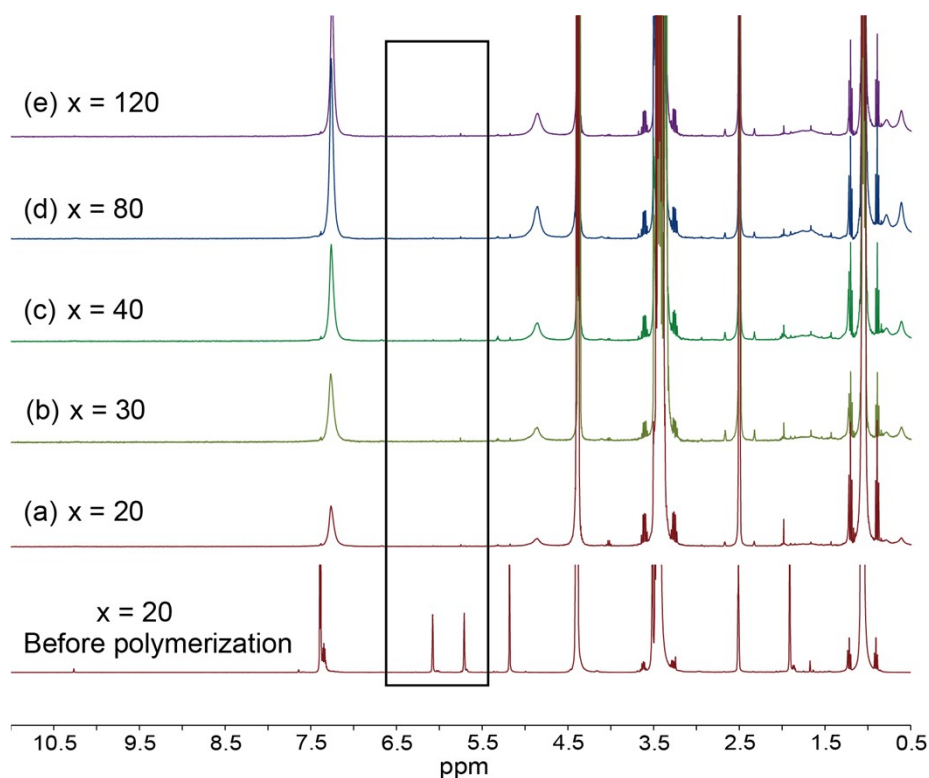


Figure S8. ^1H NMR spectra of the polymerization mixture with different target DPs of PBzMA (CL/PETTC = 1), x = 20 (a), 30 (b), 40 (c), 80 (d) and 120 (e), respectively. For each sample, 50 μL of the polymerization mixture was taken out and then added into 0.6 mL DMSO-d_6 for ^1H NMR characterization.

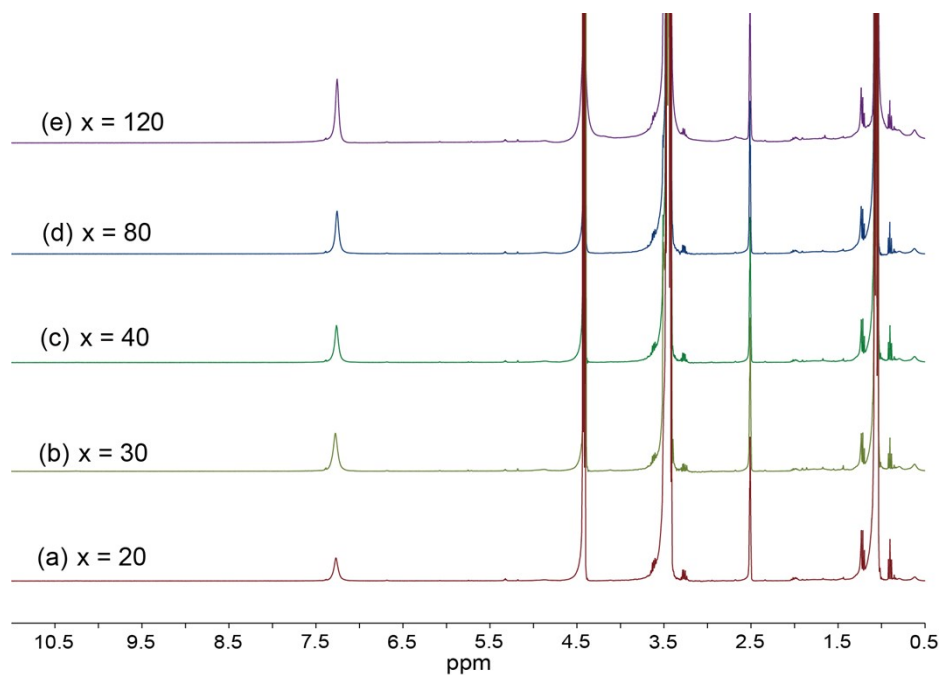


Figure S9. ^1H NMR spectra of the polymerization mixture with different target DPs of PBzMA (CL/PETTC = 2), $x = 20$ (a), 30 (b), 40 (c), 80 (d) and 120 (e), respectively. For each sample, 50 μL of the polymerization mixture was taken out and then added into 0.6 mL DMSO- d_6 for ^1H NMR characterization.

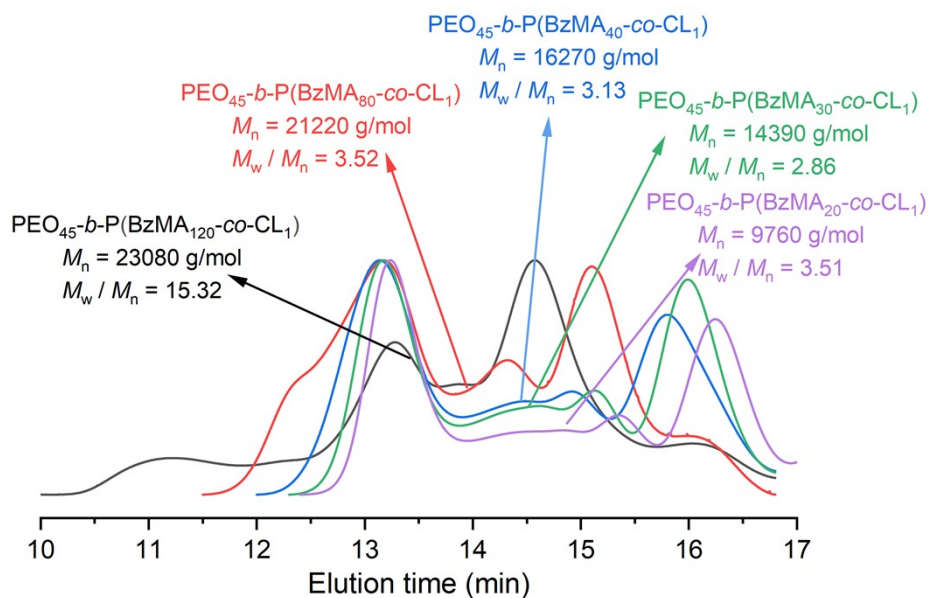


Figure S10. The GPC curves of $\text{PEO}_{45}\text{-}b\text{-P}(\text{BzMA}_x\text{-co-CL}_1)$ block copolymers ($x = 20, 30, 40, 80, 120$) with THF as eluent.

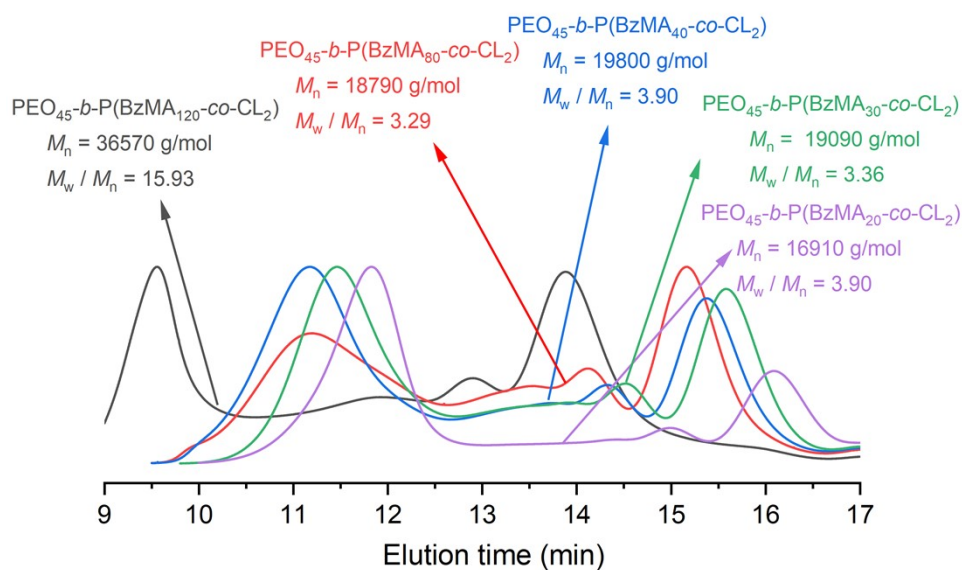


Figure S11. The GPC curves of $\text{PEO}_{45}\text{-}b\text{-P}(\text{BzMA}_x\text{-co-CL}_2)$ block copolymers ($x = 20, 30, 40, 80, 120$) with THF as eluent.

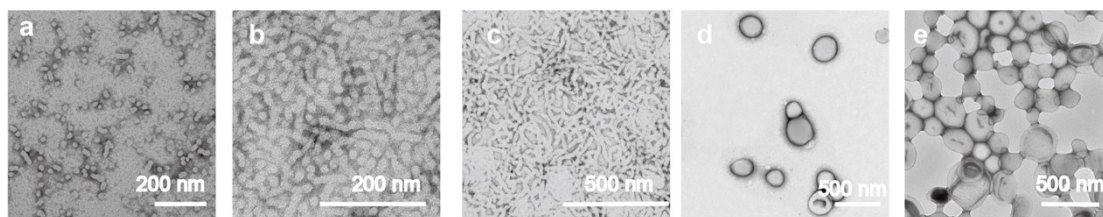


Figure S12. Transmission electron microscopy (TEM) images of PEO₄₅-*b*-P(BzMA_x-*co*-CL₁) nano-objects, x = 20 (a), 30 (b), 40 (c), 80 (d) and 120 (e), respectively.

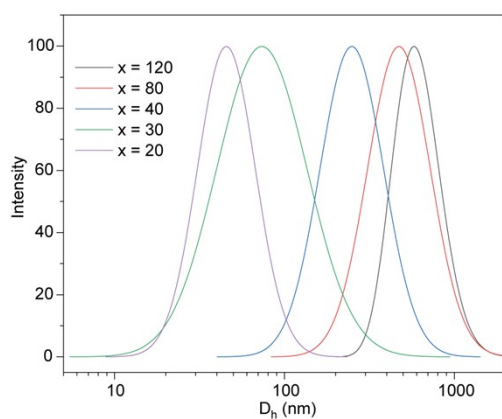


Figure S13. The DLS data of PEO₄₅-*b*-P(BzMA_x-*co*-CL₁) nanoparticles (x = 20, 30, 40, 80, 120) in ethanol/water mixture (w/w = 80/20).

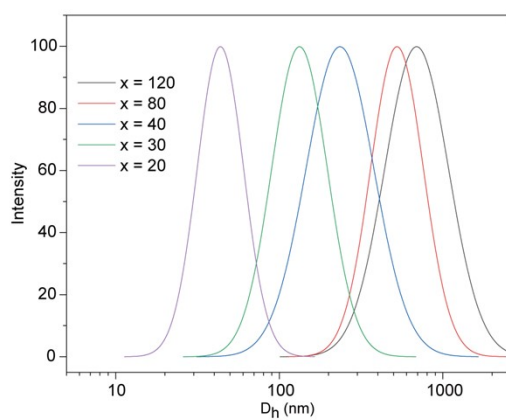


Figure S14. The DLS data of PEO₄₅-*b*-P(BzMA_x-*co*-CL₂) nanoparticles (x = 20, 30, 40, 80, 120) in ethanol/water mixture (w/w = 80/20).

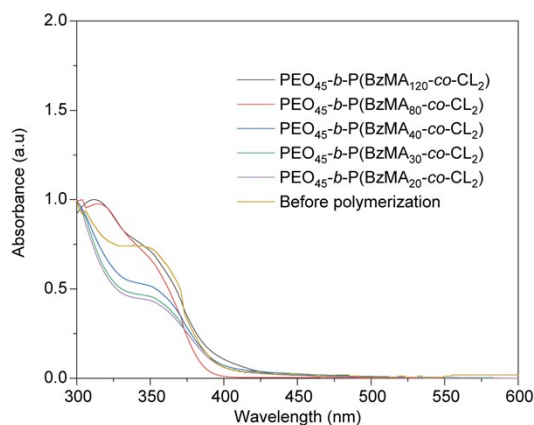


Figure S15. Normalized UV-vis absorption spectra of $\text{PEO}_{45}\text{-}b\text{-P}(\text{BzMA}_x\text{-}co\text{-CL}_2)$ nano-objects ($x = 20, 30, 40, 80, 120$) in ethanol/water mixture ($w/w = 80/20$).

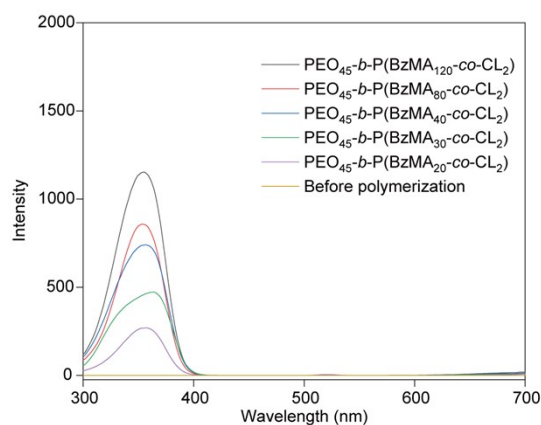


Figure S16. Excitation spectra of $\text{PEO}_{45}\text{-}b\text{-P}(\text{BzMA}_x\text{-}co\text{-CL}_2)$ nano-objects ($x = 20, 30, 40, 80, 120$) in ethanol/water mixture ($\lambda_{em} = 520$ nm).

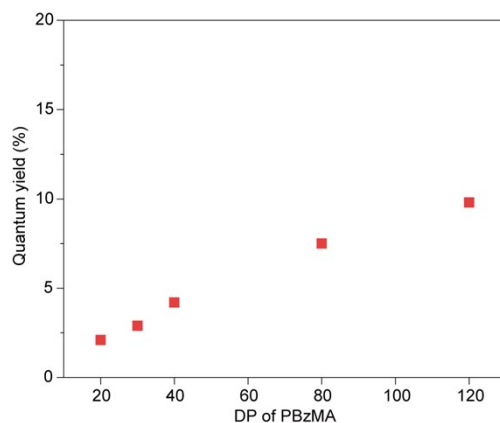


Figure S17. Relative phosphorescence quantum yields of PEO₄₅-*b*-P(BzMA_{*x*}-*co*-CL₂) nano-objects (*x* = 20, 30, 40, 80, 120) in ethanol/water mixture (w/w = 80/20).

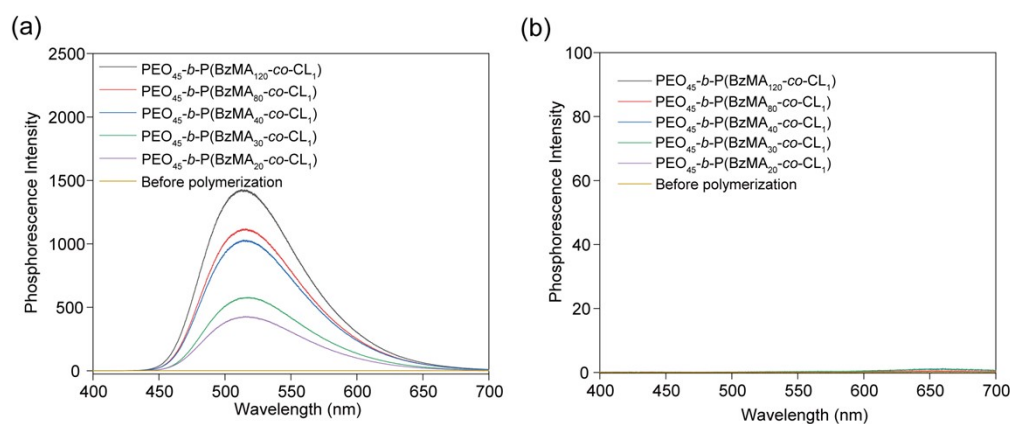


Figure S18. The phosphorescence spectra of PEO₄₅-*b*-P(BzMA_{*x*}-*co*-CL₁) nanoparticles (*x* = 20, 30, 40, 80, 120) in ethanol/water mixture (w/w = 80/20) (a) and THF (b).

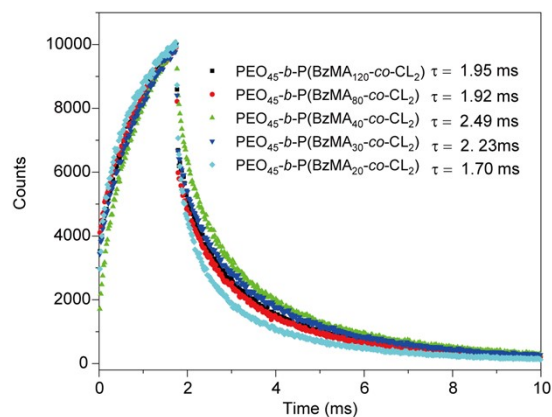


Figure S19. The phosphorescence decay traces of $\text{PEO}_{45}\text{-}b\text{-P}(\text{BzMA}_x\text{-}co\text{-}\text{CL}_2)$ nanoparticles ($x = 20, 30, 40, 80, 120$) in ethanol/water mixture ($w/w = 80/20$).

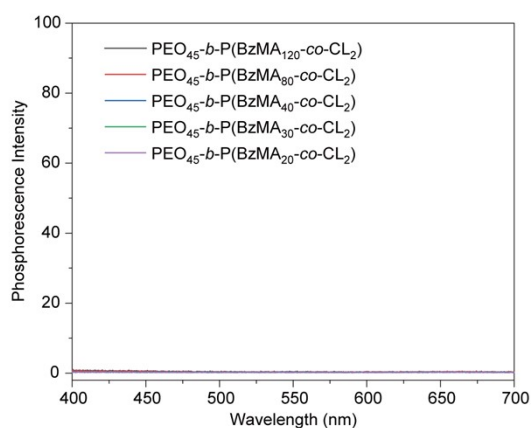


Figure S20. The phosphorescence spectra of $\text{PEO}_{45}\text{-}b\text{-P}(\text{BzMA}_x\text{-}co\text{-}\text{CL}_2)$ nano-objects ($x = 20, 30, 40, 80, 120$) in ethanol/water mixture ($w/w = 80/20$) under air.

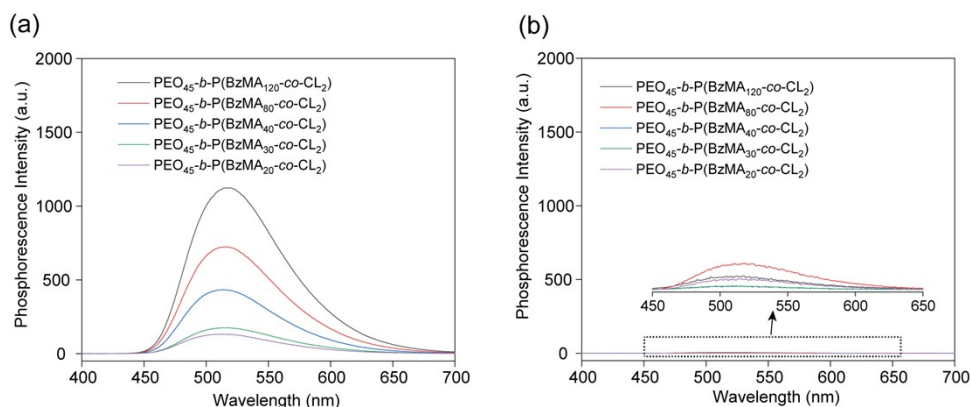


Figure S21. The phosphorescence spectra of $\text{PEO}_{45}\text{-}b\text{-P}(\text{BzMA}_x\text{-}co\text{-CL}_2)$ nano-objects ($x = 20, 30, 40, 80, 120$) in solid state (a) in vacuum and (b) in air.

Reference

- [1] Wen, S. P.; Saunders, J. G.; Fielding, L. A., Investigating the influence of solvent quality on RAFT-mediated PISA of sulfonate-functional diblock copolymer nanoparticles. *Polym. Chem.*, **2020**, *11*, 3416-3426.
- [2] Yu, Y.; Kwon, M. S.; Jung, J.; Zeng, Y.; Kim, M.; Chung, K.; Gierschner, J.; Youk, J. H.; Borisov, S. M.; Kim, J., Room-Temperature-Phosphorescence-Based Dissolved Oxygen Detection by Core-Shell Polymer Nanoparticles Containing Metal-Free Organic Phosphors. *Angew. Chem. Int. Ed.*, **2017**, *56*, 16207-16211.